Cross-section measurement for the energy pooling collisions: $Cd(5p\ ^3P_1)+Cd(5p\ ^3P_1)\rightarrow Cd(5d\ ^3D_J)+Cd(5s\ ^1S_0)$

S. Barsotti,[1] F. Fuso,[1] A. F. Molisch,[2] and M. Allegrini[1,*]
[1]*Istituto Nazionale per la Fisica della Materia, Dipartimento di Fisica, Università di Pisa, Piazza Torricelli 2, I-56126 Pisa, Italy*
[2]*Institut für Nachrichtentechnik und Hochfrequenztechnik, Technische Universität Wien, Gusshausstrasse 25/389, A-1040 Wien, Austria*
(Received 17 April 1997)

Energy pooling collisions of two cadmium atoms in the state $5s5p\ ^3P_1$ have been investigated under pulsed laser excitation and cross sections have been measured for the production of atoms in the $5s5d\ ^3D_J$ states. We have obtained the values $(1.3\pm0.6)\times10^{-16}$, $(1.1\pm0.5)\times10^{-16}$, and $(0.7\pm0.4)\times10^{-16}$ cm^2 for $J=1,2,3$, respectively. The effects of the radiation trapping phenomenon, important both in the cross-section determination and in the evaluation of the Cd atom density in the sealed cell used in the experiment, have been taken into account through numerical solutions of the radiation diffusion equation in the specific conditions of our experiment. [S1050-2947(98)05102-6]

PACS number(s): 34.90.+q, 32.50.+d

I. INTRODUCTION

The phenomenon of energy pooling (EP) takes place during the collision of two electronically excited atoms, yielding one highly excited atom and one in a low-lying state, typically the ground state. This phenomenon was observed for the first time in 1976 in sodium atoms [1], and it has been extensively investigated in alkali vapors. More recently, analysis of EP processes was extended to atoms with two valence electrons belonging to the IIA column, Mg [2], Ca [3], Sr [4], Ba [5,6], and to the IIB column, Zn [7], Cd [8], and Hg [9,10].

For Cd atoms, of interest in this work, it is relatively easy to observe $5p\ ^3P_1+5p\ ^3P_1$ energy pooling collisions. It must be noted that the excited level $5p\ ^3P_1$ is connected to the ground state $5s\ ^1S_0$ only through an intercombination transition, and that the $5p\ ^3P_1$ level is metastable (natural lifetime $\tau=2.46\ \mu$s [11]), but the measurement of the relevant cross sections is not easy. Umemoto *et al.* [8] have observed and analyzed the time behavior of the fluorescence signals from Cd levels populated by energy pooling collisions as a function of the pressure of different buffer gases present in the cell along with Cd vapors, but they have not reported any cross-section measurements. Also in our laboratory preliminary observations of EP in Cd vapors were easily performed using a heat-pipe cell filled with the metal [12], but it was not possible to give any quantitative result.

In this work we present the measurement of the EP cross sections for the processes

$$Cd(5p\ ^3P_1)+Cd(5p\ ^3P_1)\rightarrow Cd(5d\ ^3D_J)+Cd(5s\ ^1S_0)+\Delta E, \quad (1)$$

with $J=1,2,3$, and $\Delta E=(4-5)k_BT$ at the typical temperatures of our experiment ($T\sim500$ K). Figure 1 shows a sketch of the energy levels relevant in the experiment.

Cadmium atoms contained in a sealed quartz cell were excited on the intercombination transition using a pulsed laser beam tuned on 3261 Å. Both the intensity of the fluorescence spectra and the time behavior of the emission from Cd excited states were acquired. The rate coefficients, $k^{(EP)}$, and the cross sections, $\sigma^{(EP)}$, for the EP processes (1) were derived from the fluorescence data by solving a rate equation

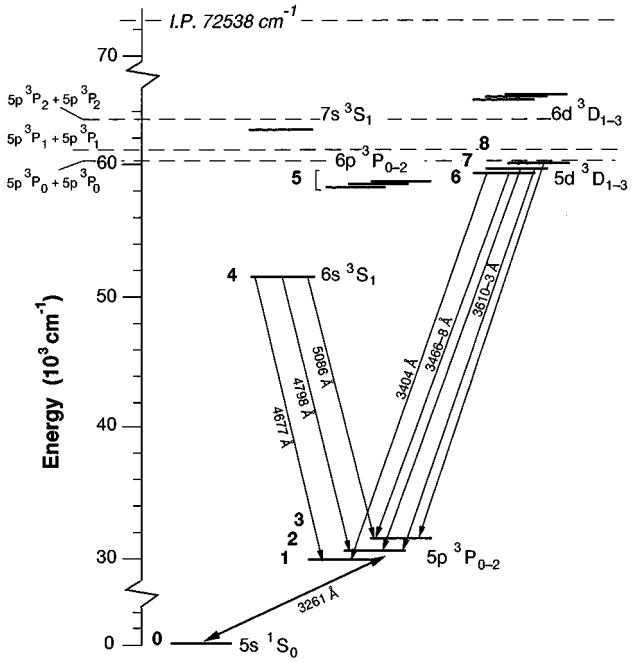

FIG. 1. Sketch of the Cd energy levels relevant in the experiment. The numbers typed in bold characters represent the level identification used in the text. The dashed horizontal line indicates the ionization energy for Cd atoms. The arrows represent the transitions of the triplet system observed in the experiment at $T=570$ K (see Table I), marked in the diagram along with their wavelength; the double arrow represents the excited intercombination transition $5s\ ^1S_0\rightarrow5p\ ^3P_1$.

*Also at Dipartimento di Fisica della Materia e Tecnologie Fisiche Avanzate, Università di Messina, Salita Sperone 31, I-98166 Sant'Agata, Messina, Italy.

system for the Cd levels involved in the experiment. The effects of the radiation trapping phenomenon, which takes place in the cell at the typical temperatures of our experiment, were taken into account in the cross-section evaluation by carrying out numerical solutions of the radiation diffusion equation in the effective conditions of the experiment. In addition, the lengthening of the intercombination transition fluorescence decay time produced by the radiation trapping allowed us to accurately derive the atom density in a way independent of the cell temperature measurement.

II. EXPERIMENTAL SETUP

We have used an apparatus typical for fluorescence spectroscopy experiments. Natural isotope cadmium metal was put in a a sealed quartz cell (14 mm radius, 180 mm length) evacuated with a turbo pump (residual pressure $< 10^{-8}$ Pa), and filled with a getter pill (an alloy of zirconium, vanadium, and iron, mod. ST707 from SAES Getters [13]), employed to absorb the residual impurities inside the cell. Since energy pooling collisions in Cd are evident at high particle densities, attainable at relatively large temperatures, we placed the cell in an electrically heated oven able to reach temperatures T greater than 800 K, with a temperature stability within 1 K. The oven was made of stainless steel, covered by an insulator (Pyrotek) withstanding up to 1100 K. Quartz windows were used for laser irradiation of the vapor and fluorescence collection.

Excitation of the $5p\ ^3P_1$ state was accomplished by using a dye laser (FL2002 Lambda Physik) pumped by a XeCl excimer laser (EMG101 MSC Lambda Physik). The attainment of stable laser pulses at 3261 Å required a careful alignment of the laser and the use of a relatively low concentration ($10^{-3}M$) of PTP dye in dioxane, which led to a maximum output energy $E_{L,\max}\sim 100$ μJ. This pulse energy was checked to be large enough to saturate the $5s\ ^1S_0 \rightarrow 5p\ ^3P_1$ transition (saturation threshold ~ 80 μJ, as determined by observing the fluorescence intensity of the intercombination transition). A beam splitter was used to send part of the laser beam to a photodiode in order to supply a trigger signal to the data acquisition system and to monitor the energy of the dye laser pulse, that remained stable within 10% on a pulse to pulse basis. The pulse duration was 10 ns full width at half maximum, and the laser bandwidth was 16 GHz, enabling excitation of the entire Doppler distribution.

Laser radiation was focused inside the vapor cell by a 560-mm focal length lens, producing a $\lesssim 0.1$ mm^2 area focal spot. The fluorescence emission from a region close to the entrance window (distance $\sim$ 5 mm) was collected at right angles by an achromatic lens and analyzed by a monochromator (HR 640 Jobin-Yvon, 640-mm focal length, 1200 g/mm grating) in the spectral range 3000–7500 Å. We note that, due to the collection geometry, our system collected not all light emerging from the outer regions of the vapor cell. Detection of the fluorescence signal was accomplished by either an intensified gateable optical multichannel analyzer (OMA PAR IRY 1000 G/BR, 1000 pixels), or a photomultiplier (Hamamatsu R955, 2.2 ns rise time) connected to a digital oscilloscope (Lecroy9400, 100 MS/s), for spectra acquisition or time-resolved measurements, respectively. The detectors were both connected to a PC for data storage and subsequent analysis. The spectral response of the collection and detection apparatus was determined by recording a blackbody spectrum produced by a quartz-iodine lamp [14]. The spectral resolution of the apparatus, depending on the monochromator slit width, was $\lesssim 1$ Å.

The absolute density of the cadmium vapor, n, was obtained following the standard method of measuring the cell temperature by a k-type thermocouple and employing the Nesmeyanov tables [15] to deduce the particle density. Measurements repeated in different points of the cell revealed that the temperature was not uniform (maximum deviation $\sim 1\%$). The uncertainty in the measurement of the effective vapor temperature along with the nonlinear character of the vapor pressure curves [15] led to an overall error in the particle density of the order of 20%. Since the particle density is a crucial parameter in the experiment, we have also derived it in a way independent of temperature measurements, starting from the lengthening in the decay time of the intercombination transition produced by the radiation trapping phenomenon. As discussed in Sec. IV A, this procedure enabled a reduction of the uncertainty in the atom density determination to $\sim 10\%$.

III. RESULTS

At first, fluorescence spectra were recorded with the multichannel detector (OMA) for an immediate identification of the Cd excited states from which we observed emission. The spectra exhibited peaks other than the resonance excited intercombination transition only at temperatures greater than ~ 560 K. At $T=570$ K, corresponding to a Cd density $n=(9.0\pm 0.1)\times 10^{14}$ cm^{-3}, the lines listed in Table I were detected. We clearly observed emission from the $5p\ ^3D_J$ and from the $6s\ ^3S_1$ states, henceafter referred as $5D$ and $6S$, respectively, decaying to the $5p\ ^3P_{J'}$ levels. These transitions are marked with an arrow in Fig. 1, along with their wavelengths. Assuming the $5D$ levels populated through EP collisions, as will be confirmed in the following, the population of the $6S$ state can be attributed to the radiative cascade $5D \rightarrow 6P \rightarrow 6S$. The intermediate transitions could not be observed, since their wavelengths, approximately 9 μm and 1.4 μm, respectively, are outside the detection range of our apparatus. In addition, the transition $5d\ ^1D_2 \rightarrow 5p\ ^1P_1$ of the singlet system was also weakly detected. The energy defect ΔE of the $5d\ ^1D_2$ is approximately $5k_BT$ at 570 K, only slightly larger than that of the $5d^3D_J$ states. Thus, EP can be invoked also for the population of the $5d\ ^1D_2$ state. However, due to the weakness of the fluorescence signal ($\lesssim 0.02$ times the fluorescence coming from the $5D$ states), which suggests an almost negligible population of the upper level, this transition was not considered in the interpretation of the experimental results of Sec. IV B.

For a further increase of the temperature, the intensities of the peaks increased and new lines appeared. At $T=635$ K, corresponding to a Cd density $n=(1.0\pm 0.1)\times 10^{16}$ cm^{-3}, the transitions reported in Table II were clearly detected, beside those listed in Table I, indicating that at this higher temperature the $6d\ ^3D_J$ and $7s\ ^3S_1$ states (henceafter indicated as $6D$ and $7S$, respectively) are populated.

After spectra acquisition, an analysis of the time behavior of the fluorescence emission was carried out in order to de-

TABLE I. List of the transitions observed at $T=570$ K [corresponding to a Cd density $n=(9.0\pm0.1)\times10^{14}$ cm^{-3}].

$\lambda_{i\to j}$ (Å)	Transition $i\to j$	E_i (cm^{-1})	E_j (cm^{-1})
3261	$5\,^3P_1\to5\,^1S_0$	30656	0
3404	$5\,^3D_1\to5\,^3P_0$	59486	30114
3466	$5\,^3D_2\to5\,^3P_1$	59498	30656
3468	$5\,^3D_1\to5\,^3P_1$	59486	30656
3610	$5\,^3D_3\to5\,^3P_2$	59516	31827
3613	$5\,^3D_2\to5\,^3P_2$	59498	31827
4677	$6\,^3S_1\to5\,^3P_0$	51484	30114
4798	$6\,^3S_1\to5\,^3P_1$	51484	30656
5086	$6\,^3S_1\to5\,^3P_2$	51484	31827
6440	$5\,^1D_2\to5\,^1P_1$	59220	43692

termine, through time integration of the acquired signals, the fluorescence intensity corresponding to each observed line. In addition, the time-resolved analysis provided information on the population mechanisms for the Cd excited states. By comparing the rise and decay times of the fluorescence signal for different transitions, it was possible to have an initial idea of the process responsible for the population of the excited states. As an example, Fig. 2 shows the fluorescence signals acquired at $T=635$ K, corresponding to $n=(1.0\pm0.1)\times10^{16}$ cm^{-3}, at different wavelengths. In the emission from the $5D$ states [see Fig. 2(c)], the peak of the time-resolved signal is within the first ≈150 ns after the arrival of the laser pulse in the interaction region, taken as the origin ($t=0$) of the horizontal axis. The emission from the $6S$ displays instead its maximum at $t\sim500$ ns [see Fig. 2(d)]. Transitions starting from the $6D$ and $7S$ states, which are observed only at higher temperatures, exhibit a time behavior characterized by a sharp fast peak superimposed to a slow increase [see Figs. 2(a) and 2(b)], similar to that of the transition from the $6S$ state. The sharp peak was essentially due to laser light scattering on the cell walls, as confirmed by comparison with measurements performed shifting the laser wavelength out of the intercombination transition resonance. The presence of the sharp peak was particularly evident in the transitions from the $6D$ and the $7S$ states, which have a wavelength relatively close to that of the laser radiation. The contribution of the sharp peak was removed in the calculation of the fluorescence intensities as time integrals of the fluorescence signal, which will be presented in the following.

The decay of the fluorescence from $5D$ states takes place in the microsecond range, as seen in Fig. 2(c). Such a value was relatively independent of the particle density: measurements performed at lower temperatures, i.e., $T=570$ K, displayed the same decay time (within the experimental uncertainties, evaluated as $\pm10\%$) for all transitions starting from $5D$ states observed in the experiment.

The analysis of time-resolved fluorescence signals suggests that different processes are responsible for the population of the $5D$, $6S$, $6D$, and $7S$ states. The fast rise time observed for the $5D\to5P$ fluorescence is in agreement with the hypothesis of population of the upper level through EP collisions, whereas the slower rise time for the $6S\to5P$ transition suggests that the $6S$ level is populated through radiative cascade from upper-lying states. The time behavior of the transitions starting from the $7S$ and $6D$ states suggests that they are populated through mechanisms other than EP. On the other hand, EP collisions can be ruled out on the basis of energetic considerations, since the energy of the $7S$ and $6D$ states (see Table II and Fig. 1) is larger than twice the energy of the resonance excited $5P$ state, and EP collisions are not expected to occur. At the typical temperatures of the experiment, $\Delta E\simeq4k_BT$ for the $5D$ levels, whereas $\Delta E\simeq-3k_BT$, $\Delta E\simeq-10k_BT$ for the $6D$ and $7S$ levels, respectively. Due to the observed remarkable dependence on the temperature of the transitions starting from these levels, collisional processes more complex than EP can be invoked. For instance, at large Cd densities intramultiplet mixing (see Sec. IV A) could produce appreciable population of the $5p\,^3P_2$ state, which might lead, through EP collisions, to the formation of $7S$ atoms (see also Fig. 1). Moreover, we cannot rule out other processes, possibly involving ionization and plasma formation, which, at higher particle densities, could be effective in populating the high-lying states observed in the experiment. Since the primary aim of our ex-

TABLE II. List of the additional transitions observed at $T=635$ K [corresponding to a Cd density $n=(1.0\pm0.1)\times10^{16}$ cm^{-3}].

$\lambda_{i\to j}$ (Å)	Transition $i\to j$	E_i (cm^{-1})	E_j (cm^{-1})
2837	$6\,^3D_1\to5\,^3P_0$	65353	30114
2881	$6\,^3D_{2,1}\to5\,^3P_1$	65359,65353	30656
2981	$6\,^3D_{3,2}\to5\,^3P_2$	65367,65359	31827
3082	$7\,^3S_1\to5\,^3P_0$	62563	30114
3133	$7\,^3S_1\to5\,^3P_1$	62563	30656
3253	$7\,^3S_1\to5\,^3P_2$	62563	31827

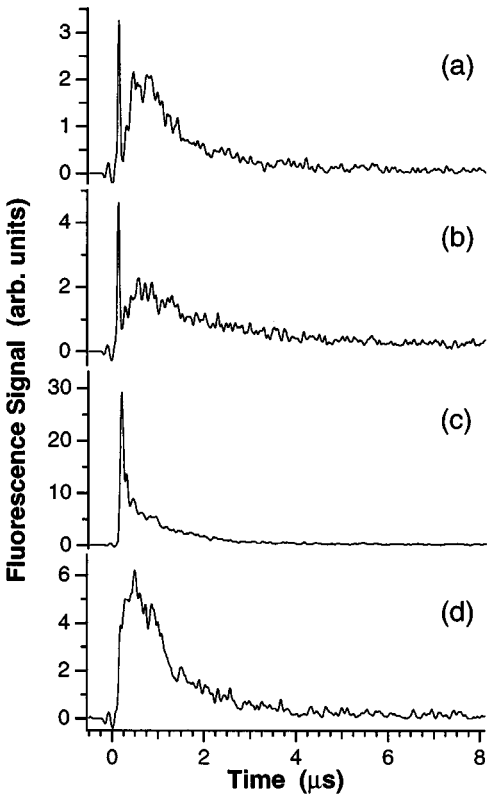

FIG. 2. Time behavior of the fluorescence signals acquired at $T = 635$ K corresponding to $n=(1.0\pm0.1)\times10^{16}$ cm^{-3} and $E_L = 50$ μJ for different transitions: $6d\ ^3D_{2,1}\rightarrow5p\ ^3P_1$ ($\lambda=2881$ Å) (a), $7s\ ^3S_1\rightarrow5p\ ^3P_1$ ($\lambda=3133$ Å) (b), $5d\ ^3D_2\rightarrow5p\ ^3P_1$ ($\lambda=3466$ Å) (c), and $6s\ ^3S_1\rightarrow5p\ ^3P_0$ ($\lambda=4677$ Å) (d).

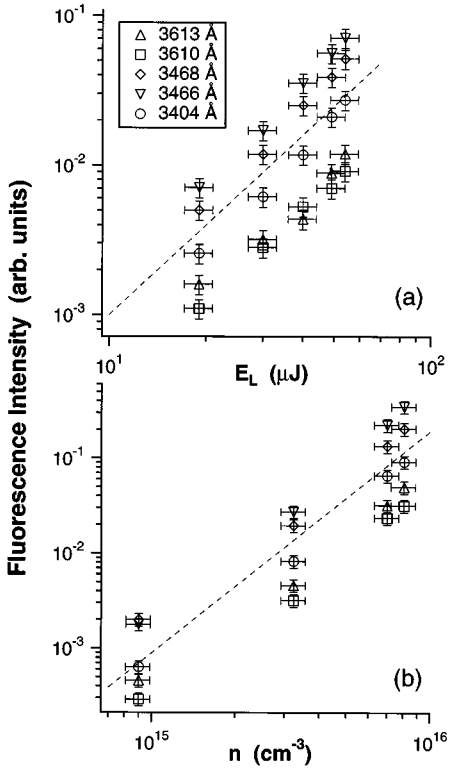

FIG. 3. Behavior of the fluorescence intensity for the transitions $5d\ ^3D_J\rightarrow5p\ ^3P_{J'}$ as a function of the dye laser energy E_L, measured at $T=590$ K, corresponding to $n=(1.4\pm0.1)\times10^{15}$ cm^{-3} (a), and of the Cd vapor density n, measured at $E_L=50$ μJ (b). The dashed lines superimposed for comparison to the experimental data represent a slope 2 behavior (a), and a slope 2.35 behavior (b).

periment is the investigation of the EP processes (1), we decided to restrict our analysis to the particle density range where the presence of these transitions is negligible, i.e., to $n\lesssim8\times10^{15}$ cm^{-3}, corresponding to $T\lesssim620$ K).

In order to further verify that the observed emission from the $5D$ states was due to EP, we analyzed the behavior of the fluorescence intensity, i.e., the integral of the fluorescence signal along all the acquired time interval (typically 20 μs, much longer than the observed lifetimes), for the transitions $5d\ ^3D_{J'}\rightarrow5p\ ^3P_J$, with $J'=1-3$ and $J=0-2$, as a function of the experimental parameters, namely, the laser pulse energy, E_L, and the vapor density, n [Figs. 3(a) and 3(b), respectively]. We varied n by changing the cell temperature in the range 570–635 K (corresponding to $n=9\times10^{14}$–9×10^{15} cm^{-3}), and E_L, by using neutral density filters, in the range 18–54 μJ, i.e., below the saturation threshold for the $5s\ ^1S_0\rightarrow5p\ ^3P_1$ transition found at $\sim$ 80 μJ. The vertical error bars reported in Figs. 3(a) and 3(b) represent the standard deviation of the fluorescence intensity measurements acquired over 100 laser shots. The error bars in the laser energy are due to fluctuations of the laser pulse, and those in the atom density account for the uncertainties in the particle density evaluation according to the method described in Sec. II.

Both the behaviors reported in a bilogarithmic scale show a slope close to 2, strengthening the hypothesis that EP collisions are the dominant mechanism for the population of the $5D$ levels. More precisely, the observed fluorescence intensity for the $i\rightarrow j$ transition, $I_{i\rightarrow j}$, where $i=6-8$ and $j=1-3$ (see Fig. 1 for the level identification) displays as a function of the laser energy a quadratic behavior within the experimental uncertainties, as confirmed by the slope 2 straight line superimposed for comparison to the experimental data (dashed line).

The behavior of the fluorescence intensity as a function of the vapor density, on the contrary, is better described by

$$I_{i\rightarrow j}\propto n^{m_{i\rightarrow j}}, \tag{2}$$

where the exponent $m_{i\rightarrow j}$ lies between 2.3 and 2.4, depending on the specific transition considered. A slope 2.35 straight line is superimposed for comparison to the data of Fig. 3(b) (dashed line). This superquadratic behavior can be (partially) ascribed to the occurrence of radiation trapping, as discussed in Sec. IV B.

IV. DISCUSSION

A. Radiation trapping effects

Before setting up the rate equation system used for the determination of the EP cross sections, it is necessary to briefly discuss the relevance of the radiation trapping phenomenon in our experiment. When this phenomenon takes

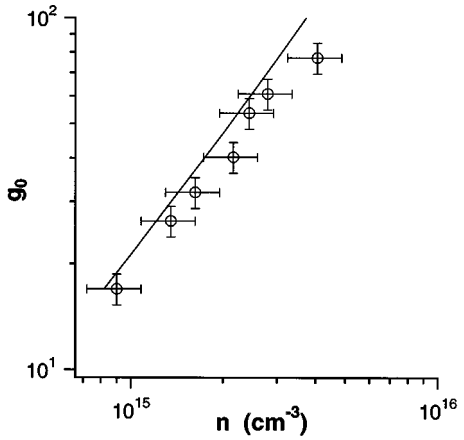

FIG. 4. Trapping factor g_0 as a function of the particle density n. The solid line represents the result of the analytical calculation discussed in the text. The open circles are values of the trapping factor, derived through an exponential best fit of the fluorescence decay for the $5p\ ^3P_1 \rightarrow 5s\ ^1S_0$ transition, as a function of the particle density obtained through temperature measurements, along with their experimental uncertainties (horizontal bars). The vertical error bars are given by the best-fit procedure.

place, the emergent radiation at late times decays like $\exp(-t/g_0\tau)$, where τ is the natural lifetime of the transition and g_0 is the lowest-order trapping factor [16].[1] Assuming a purely Doppler-broadened line at high opacities, the trapping factor for the intercombination line is [17]

$$g_0 = 1.06\ \ n\sigma_{02}[\pi \ln(n\sigma_{02})]^{0.5}, \tag{3}$$

where σ_{02} is the absorption cross section for the intercombination transition.

Equation (3) shows that the relation between particle density and the effective decay time, $g_0\tau$, is approximately linear. The particle density is thus much less sensitive to uncertainties in the lifetime measurements than in the temperature measurements, where the relation between particle density and temperature is exponential. Thanks to this feature, the analysis of the observed decay time allowed us to improve the accuracy in the determination of the density n.

It must be noted that, for the evaluation of the g_0 factor in the actual conditions of our experiment, dealing with a natural isotope sample, different isotopes displaying different spectral features, and with a broadband laser excitation, we have to take into account both isotope and hyperfine splitting of the atomic sample. As a consequence, Eq. (3) must be replaced by a more complex expression. Indeed, we evaluated the Holstein equation for the $5p\ ^3P_1$ Cd density, denoted as n_2 according to our level identification (see Fig. 1) by reducing it to an algebraic eigenvalue problem [18] and computing the lowest-order eigenvalue. Figure 4 shows the relation between the trapping factor g_0 and the particle density n resulting from our calculations. In the same graph, experimental g_0 values found through an exponential best fit of the intercombination fluorescence decay acquired at different temperatures are reported (open circles) as a function of the density derived from the temperature measurements according to the Nesmeyanov tables. The vertical error bars reflect the uncertainties in the decay time derived from the best fit procedure, whereas the horizontal error bars are mainly affected by the uncertainty in the temperature measurements in different points of the cell. Except the data at the largest particle density, which is probably affected to a larger extent by the ambiguous determination of the actual vapor temperature, the behavior of the trapping factor g_0 as a function of the particle density derived from the experimental data is in agreement with the theoretical results within approximately 10%, which has been taken as the uncertainty in the particle density measurement. In addition, the data reported in Fig. 4 demonstrate the occurrence of radiation trapping even at the lowest particle density range exploited in the present work, and stress the need for the development of theoretical methods to account for this effect.

Besides the discussion of the radiation trapping in the intercombination transition lifetime, we have to consider the effects on the excited-state density, and thus on the rate equation we used to derive the EP cross sections. As previously stated, radiation trapping causes the excitation to stay longer in the vapor. This offers a larger chance for the $5p\ ^3P_1$ atoms to collide and thus reach a higher state. In order to find the distribution of $5p\ ^3P_1$ atoms at all times, we first had to compute the initial distribution of excited atoms. This was rather straightforward, because the exciting pulse is much shorter than the natural lifetime, and no trapping occurs during the excitation. We have assumed a Maxwell-Boltzmann distribution for the ground state atoms, and supposed that no velocity-changing collisions occur during the laser shot, a reasonable approximation owing to the short duration of the pulse. We have then divided the ground-state atoms into velocity subgroups, each of which can absorb laser light in a narrow frequency band, and solved the Beer-Lambert equation coupled to the rate equation for each velocity subgroup. The excited-state densities of each velocity subgroup have been finally added up to obtain the total $5p\ ^3P_1$ density, n_2, at the end of the pulse, i.e., at the beginning of the decay stage. For the evaluation of n_2 at the end of the laser pulse, we have assumed a negligible population of the upper states as well as of the $5p\ ^3P_0$ state, populated by intramultiplet mixing, as discussed in the following. The data we used for the cross-section evaluation were acquired at a laser pulse energy $E_L \simeq 100\ \mu$J, i.e., larger than the saturation threshold. In these conditions, following the method already used in Ref. [10], it is possible to derive the maximum density of the $5p\ ^3P_1$ state. In fact, the total population splits itself into the ground and the $5p\ ^3P_1$ states according to their statistical weights. Considering that our laser is linearly polarized, only the Zeeman sublevel $5p\ ^3P_1\ m=0$ can be populated. As a consequence, the maximum density of the $5p\ ^3P_1$ state turns out to be one-half of the total atom density, n.

We then had to compute the eigenmodes of the Holstein equation in the cylinder volume describing the experimental geometry. In contrast to the density measurements, where we required only the lowest-order mode, we have now to consider also early times, and thus need higher-order modes. Since a considerable part of the laser pulse is absorbed near

[1]Note that we denote as the trapping factor g_0 the inverse of the Holstein escape factor.

the entrance window, we have also to account for the geometry of the problem. Due to the invariance of the problem under rotation, the problem can be seen as two dimensional, and a cylindrical reference system (r,z) describes appropriately the collection geometry exploited in our experiment.

The $5p\ ^3P_1$ density is then

$$n_2(r,z,t)=\sum_i \sum_j \alpha_{ij}\psi_{ij}(r,z)\exp(-t/g_{ij}\tau), \qquad (4)$$

where the ψ_{ij} and g_{ij} are the ij eigenmodes and trapping factors, and the α_{ij} the expansion coefficients of the initial distribution into the eigenmodes. Trapping factors for two-dimensional geometries can be found in [19]. In addition to the trapping, we have to take the particle diffusion into account. This is done by the technique described in [20].

It must be noted that population of the $5p\ ^3P_0$ and $5p\ ^3P_2$ can occur to some extent through intramultiplet mixing collisions. According to Refs. [21,22], population of the highest sublevel is expected to be negligible in the actual conditions of our experiment, whereas the rate for the population of the $5p\ ^3P_0$ state lies in the 10^{-11} cm^3 s^{-1} range. Thus, radiation trapping can affect to some extent also the fluorescence for the transitions connected to the $5p\ ^3P_0$ state (radiation trapping can be considered negligible for the transitions connected to the weakly populated $5p\ ^3P_2$ state). However, the trapping turns out to have practically a negligible effect on all transitions to the $5P$ levels for the following reasons.

As previously stated in the comment to Fig. 2, the decay of the fluorescence signal from $5D$ states takes place in the microsecond range. If no radiation trapping were present, the observed lifetime for those transitions would be approximately one-half the lifetime of the $5p\ ^3P_1$ state, that is, $\sim$1.25 μs, as expected on the basis of the rate equations ruling the process under investigation (see Sec. IV B). It must be noted that the actual value can be slightly affected by other processes, as the nonradiative transport of $5P$ atoms, which will be discussed in the following, and the finite lifetime of the $5D$ state, which leads to a double-exponential decay in the observed signals. Thus, our experimental results suggest that radiation trapping does not significantly affect the emission from the $5D$ atoms. This statement implies two considerations: (i) the radiation trapping of the intercombination line does not significantly affect the (time behavior) in the production of $5D$ atoms; (ii) the radiation trapping of the $5D\rightarrow 5P$ transitions does not affect the measurement of their (time integrated) fluorescence intensity.

Concerning the first statement, we note that $5P$ atoms created by radiation trapping, i.e., by reabsorption of the intercombination fluorescence, are spread out in space. After 2.5 μs their radial extension is, at a first approximation, $1/k_0$, where k_0 is the line-center absorption coefficient, corresponding approximately to 0.05 cm and 0.5 cm at the highest and lowest Cd densities used in our experiment, respectively. This implies that the density of $5P$ atoms created after one reemission is at least two order of magnitude lower than the density of the atoms directly excited by the laser beam, though the total number is the same. Since the $5D$ density depends quadratically on the $5P$ density, the consequence is that the total number of $5D$ atoms created because of radiation trapping of the intercombination line is very small. Furthermore, since the lifetime of the $5D$ states is small enough to produce negligible effects, even if it is somewhat increased by radiation trapping, the decay rate of the $5D\rightarrow 5P$ radiation is essentially ruled by the creation rate of the EP process, so that we find the time behavior of the $5D\rightarrow 5P$ transition practically independent of the radiation trapping. This is substantially confirmed by our measurements, which indicate that radiation trapping does not markedly affect the time behavior of the emission from $5D$ states, whereas it has a dramatic effect on the fluorescence from the $5p\ ^3P_1$ state. However, we stress that the above description is intended only to give an intuitive relation between the physical model and the experimental results, and that any residual influence of the radiation trapping for the intercombination line is included in our theoretical treatment of the problem, which will be presented in the next section.

The second point we mentioned above is that we assume that the radiation trapping of the $5D\rightarrow 5P$ transitions does not affect the measurement of their (time integrated) intensity. To justify this statement, we note as first that the $5P$ atoms remain within an ''infinite cylinder'' during the time relevant in the fluorescence emission, i.e., the first 2.5 μs. In fact, the extension of $5P$ atoms at $t=2.5$ μs at the lowest density range explored in the experiment can be estimated as $\approx$5 cm and $<$0.5 cm along the axial and radial directions, respectively. At larger particle densities the spread of the $5P$ atoms is even smaller ($\approx$0.05 cm and less than 0.05 cm at the largest densities explored in the experiment). Thus, the radial extension of the $5p\ ^3P_1$ atoms increases to, e.g., 0.5 cm in 2.5 μs, but it remains still much smaller than along the axial direction. Radiation trapping in such a configuration, well approximated by an infinite cylinder, can produce a significant influence on the emergent radiation by three effects: (i) the emission decay takes place in a longer time; as stated above, this is negligible and of no further concern if we consider only the time-integrated fluorescence intensity; (ii) the spatial redistribution of atoms, which can occur only on the scale of the cylinder diameter and is thus negligible; (iii) for a strongly branching transition, the trapping leads to a decrease in the fluorescence intensity, since, at each reemission, the excitation can decay through a different (unobserved) radiative path. Considering the transitions detected in the experiment, only the two transitions $6d\ ^3D_1\rightarrow 5p\ ^3P_{0,1}$ have a strongly branched upper state, and are thus expected to be influenced to some extent by radiation trapping. Those transitions where radiation trapping is involved are very sensitive to errors in the excited state distribution and in the branching ratios. Thus, a reliable evaluation of the radiation trapping effects for those transitions is not easy. However, in our case they are not directly involved in the EP cross-section determination, and they will be neglected in the following discussion.

B. Evaluation of the cross sections

To interpret the experimental results and to derive the values of the EP cross sections, we started from a model based on a rate equation system involving nine Cd levels (see Fig. 1). We included into the model the effects of the EP collisions, of the spontaneous and stimulated radiative emis-

sions, and of nonradiative quenching processes. We made some approximations, by considering the triplet $6p\ ^3P_J$, with $J=0,1,2$, as a single level (denoted as 5, see Fig. 1) and a nonradiative quenching process with the same rate for each level. The cross section for the quenching was determined based on the geometrical cross section (Cd radius=1.58 Å [23]).

Since the density of the higher states considered in our system is much smaller than the $5P$ density, the rate equations are effectively decoupled, i.e., the production rate $k_{2\to i}^{(\mathrm{EP})} n_2^2(r,t)$ for the higher state i, with $i=6-8$ (see Fig. 1) can be viewed as a given excitation term for the computation of the higher-state densities, and can be neglected in the rate equation of the $5P$ atoms. Since the pooling cross section is smaller than the quenching cross section, the (nonlinear) pooling rates are certainly smaller than the (linear) decay processes at all densities considered in the present work. This leads to a considerable simplification; the rate equation that describes the behavior of the population via EP of one of the $5D$ states, n_i, with $i=6-8$ (see Fig. 1), becomes

$$\frac{dn_i}{dt}=-\sum_{k<i} A_{i\to k} n_i+\frac{1}{2}k_{2\to i}^{(\mathrm{EP})} n_2^2-k^{(Q)} n_i n_0, \tag{5}$$

where $A_{i\to k}$ is the Einstein coefficient for spontaneous emission from the state i to all k states connected through radiative transitions, $k^{(Q)}$ is the quenching rate coefficient for nonradiative processes, and $k_{2\to i}^{(\mathrm{EP})}$ is the EP rate coefficient for the population of the i level due to collisions between atoms in the $5p\ ^3P_1$ state. It must be noted that, in principle, the $A_{i\to k}$ coefficients should be modified to account for radiation trapping of transitions connected to the $5P$ states, but, as discussed in the previous section, this effect is negligible in our experimental conditions. To simplify notation, we have dropped the functional dependence on space and time in the terms entering Eq. (5). However, we stress that the rate equation system ruling level population in our experiment is valid locally, and that its solution has to be performed accounting for the space dependence. The $\frac{1}{2}$ factor in $k^{(\mathrm{EP})}$ is due to the fact that we have a homonuclear collision involving two partners of the same species [24,25]. The self quenching can be neglected, because at the typical temperatures of our experiment it is two orders of magnitude smaller than the radiative decay. We have shown in Sec. IV A that the radiation trapping has practically no effect on the density of the $5D$ atoms. We can thus neglect it completely at this stage of the discussion.

Furthermore, the radiative decay of the upper states is much faster than the decay of the $5P$ atoms, so that, at any time, we are essentially in steady state equilibrium between those two levels, and the upper state density can be computed from

$$n_i=\frac{\frac{1}{2}k_{2\to i}^{(\mathrm{EP})} n_2^2}{\sum_{k<i} A_{i\to k}}. \tag{6}$$

Finally, we find the time integrated fluorescence intensity as

$$I_{i\to j}=\frac{\Omega\varepsilon}{4\pi}\alpha_{i\to j} h\nu_{i\to j} A_{i\to j}\int_0^\infty\int_V n_i(\mathbf{r},t)d\mathbf{r}\,dt, \tag{7}$$

where V describes the volume in the cell observed by the monochromator, Ω is the solid angle for radiation collection, ε is the quantum efficiency of the detector, $\alpha_{i\to j}$ is the experimental apparatus response at the wavelength corresponding to the $i\to j$ transition, and $\nu_{i\to j}$ is the frequency of the transition.

For the intercombination line, the radiation trapping has to be included, and the observed intensity is computed from

$$I_{2\to 0}=\frac{\Omega\varepsilon}{4\pi}\alpha_{2\to 0} h\nu_{2\to 0} A_{2\to 0}\int_0^\infty\int_V\int_{-\infty}^{\infty} n_2(\mathbf{r},t)\Phi(x)\exp[-\xi_{20}(\mathbf{r},x)]dx\,d\mathbf{r}\,dt, \tag{8}$$

where $\xi_{20}(\mathbf{r},x)$ denotes the opacity for the intercombination line from point $\mathbf{r}$ to the detector, x is the (normalized) transition frequency, and Φ is the emission line shape of the intercombination line, normalized so that its integral is unity.

Experimental uncertainties about the collection angle and detector sensitivity can be greatly reduced by considering only the ratio between the observed fluorescence intensity for one of the transitions $5\ ^3D_J\to 5\ ^3P_{J'}$ ($i\to j$, with $i=6-8$ and $j=1-3$) and the intercombination transition $5\ ^3P_1\to 5\ ^1S_0$ ($2\to 0$):

$$\frac{I_{i\to j}}{I_{2\to 0}}=\frac{\alpha_{i\to j}}{\alpha_{2\to 0}}\frac{\nu_{i\to j}}{\nu_{2\to 0}}\frac{A_{i\to j}}{A_{2\to 0}}\frac{\int\int n_i(\mathbf{r},t)d\mathbf{r}\,dt}{\int\int\int n_2(\mathbf{r},t)\Phi(x)\exp[-\xi_{20}(\mathbf{r},x)]dx\,d\mathbf{r}\,dt}. \tag{9}$$

Using Eq. (6), Eq. (9) can be written as

$$k_{2\to i}^{(\mathrm{EP})}=2\frac{I_{i\to j}}{I_{2\to 0}}\frac{\alpha_{2\to 0}}{\alpha_{i\to j}}\frac{\nu_{2\to 0}}{\nu_{i\to j}}\frac{\Sigma_{k<i}A_{i\to k}}{A_{i\to j}}A_{2\to 0}\frac{\int\int\int n_2(\mathbf{r},t)\Phi(x)\exp[-\xi_{20}(\mathbf{r},x)]dx\,d\mathbf{r}\,dt}{\int\int n_2^2(\mathbf{r},t)d\mathbf{r}\,dt}. \tag{10}$$

Equation (10) is the basic equation we have used to derive the rate coefficients for the processes of Eq. (1) from the experimental fluorescence intensities. The radiation trapping is taken into account by using the correct spatiotemporal distribution of the excited state density, and the self-absorption of the emergent radiation, described by the exponential factor.

By introducing the mean interatomic velocity:

TABLE III. EP cross sections for the $5\,^3D_J$ levels measured at $T=570$ K.

Level	$\sigma^{(EP)}$ (cm^2)
$5\,^3D_1$	$(1.3\pm0.6)\times10^{-16}$
$5\,^3D_2$	$(1.1\pm0.5)\times10^{-16}$
$5\,^3D_3$	$(0.7\pm0.4)\times10^{-16}$

$$\langle v\rangle=\sqrt{\frac{8k_BT}{\pi\mu}}, \tag{11}$$

where μ is the reduced mass of the colliding atom system, we can deduce the values of the EP cross sections by

$$\sigma^{(EP)}=\frac{k_{2\to i}^{(EP)}}{\langle v\rangle}. \tag{12}$$

The numerical values of $\sigma^{(EP)}$ obtained at $T=570$ K and $E_L=100$ μJ are reported in Table III.

As a check for the validity of our analysis and as a confirmation for the role played by the radiation trapping, it is interesting to compute the ratio of the double integrals in Eq. (9), i.e., the ratio of the observed intensities, as a function of the particle density n. If there were no radiation trapping, then the intensity of the intercombination line would increase linearly with n, and the fluorescence from the $5D$ states quadratically. In other words, the difference between the exponents introduced in Eq. (2) $(m_{i\to j}-m_{2\to0})$ would be unity. Due to the radiation trapping, the intercombination line intensity increases sublinearly, because the trapping redistributes the excited-state atoms in the cell volume, leading to a decrease of the $5P$ atoms in the fluorescence collection region (close to the entrance window) compared to the ideal situation where radiation trapping is absent. Thus, the $m_{2\to0}$ exponent ruling the behavior of the intercombination fluorescence as a function of the density tends to decrease. The theoretical analysis of the radiation trapping based on the method described in Sec. IV A gives $m_{2\to0}\simeq0.9$. Figure 5, reporting the fluorescence intensity of the intercombination transition $I_{2\to0}$ (open circles) measured as a function of the vapor density n along with the theoretical prediction (line), demonstrate a good agreement between experiment and theory.

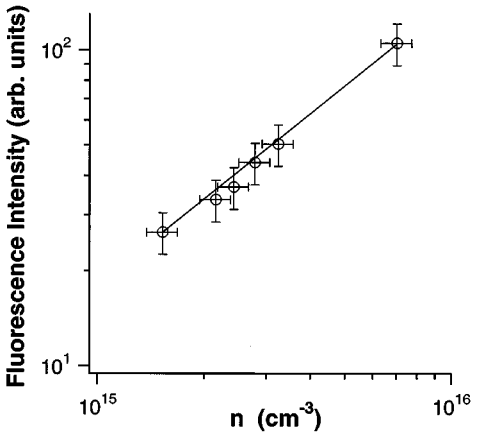

FIG. 5. Fluorescence intensity of the $5p\ ^3P_1\to5s\ ^1S_0$ transition as a function of the particle density (circles), along with their experimental error. The solid line represents the result of the theoretical simulation obtained as discussed in the text. A multiplicative factor has been used to fit the experimental data.

The emission intensity from the upper states, $I_{i\to j}$, on the contrary, increases faster than quadratically because the trapping of the intercombination line increases the chance of pooling collisions. As shown in Sec. III [see Eq. (2) and Fig. 3(b)], the exponent $m_{i\to j}$ ruling the functional dependence of the observed fluorescence intensity for the transitions from $5D$ states is between 2.3 and 2.4. From our computations, the theoretical $m_{i\to j}$ turns out to be $\simeq$ 2.6. Thus, the difference $(m_{i\to j}-m_{2\to0})$ evaluated theoretically is approximately 1.7, to be compared with the $\sim$ 1.4 value found in the experiment. This $\sim$ 20% deviation is probably due to an incomplete knowledge of the effective shape and size of the observation region used in our treatment of the radiation trapping, which relies on a correct estimate of the fluorescence collection geometry.

Despite this discrepancy, the above presented analysis of the emerging fluorescence intensity as a function of the vapor density confirms the role played by radiation trapping in our experiment, and the reasonable agreement between theory and experiment indicates indirectly the validity of the method we have adopted to account for radiation trapping effects.

Finally, the estimation of the uncertainty for our $\sigma^{(EP)}$ measurements deserves some discussion. Various dominant factors affect the $\sigma^{(EP)}$ determination. At first, the indirect evaluation of the density n_2 based on the measurement of the particle density is expected to produce an important uncertainty, which we have estimated of the order of 40%. In fact, the occurrence of saturation for the intercombination transition, which represents the basis of our determination of the maximum n_2 density (see Sec. IV A), is difficult to assess from the experimental point of view. In addition, we must take into account experimental errors in the fluorescence intensity measurements and those due to the fluctuations in the laser pulse energy, which can be estimated as 10%. There are also some uncertainties in the values of the Einstein coefficients (not always clearly specified in the literature) entering our cross-section calculation, that we assumed to be of the order of 10%. Moreover, since our results rely on a correct description of the radiation trapping effects, we have to consider also the errors made in the theoretical evaluation of this phenomenon. Although a quantitative estimation is rather difficult, we can take the above presented discrepancy between theoretical predictions and experimental data ($\sim$20%) as an additional uncertainty related to our calculation of the radiation trapping effect, which leads to an estimation of the overall uncertainty in $\sigma^{(EP)}$ of the order of $\pm$50%.

V. CONCLUSIONS

In the present work we have quantitatively investigated the energy pooling processes occurring in pure cadmium vapors contained in a sealed cell under pulsed laser excitation resonant with the intercombination transition $5s\ ^1S_0\to5p\ ^3P_1$, and we have derived the cross sections for the

reactions of Eq. (1). We have based our analysis on a rate equation model, which accounts for the dominant radiative and nonradiative mechanisms taking place in our experimental conditions. In addition, we have considered the effects of the radiation trapping, which turns out to play an important role in the experiment, through numerical solutions of the radiation diffusion equations performed in the specific conditions of our experiment.

ACKNOWLEDGMENTS

This work was supported by EC Network Grant No. ERBCHRXCT 930344. M. Badalassi prepared the quartz cell and H.B. Van Linden van den Heuvell and F.B. de Jong filled it with the proper getter. We gratefully acknowledge them, as well as S. Gennai and M. Montanari who constructed the oven.

[1] M. Allegrini, G. Alzetta, A. Kopystynska, L. Moi, and G. Orriols, Opt. Commun. **19**, 96 (1976).
[2] W. H. Breckenridge, W. L. Nickolai, and J. Stewart, J. Chem. Phys. **74**, 2073 (1981).
[3] C. Gabbanini, A. Lucchesini, and S. Gozzini, J. Phys. B **27**, 4643 (1994).
[4] S. F. Kelly, M. Harris, and A. Gallagher, Phys. Rev. A **38**, 1225 (1988).
[5] J. A. Neuman, A. Gallagher, and J. Cooper, Phys. Rev. A **50**, 1292 (1994).
[6] G. De Filippo, S. Guldberg-Kjær, S. Milošević, and J. O. P. Pedersen, J. Phys. B **29**, 2033 (1996).
[7] B. Cheng, Z. Li, Y. Yang, J. Zhu, and D. Zhang, Opt. Commun. **86**, 465 (1991).
[8] H. Umemoto, J. Kikuma, A. Masaki, and S. Sato, Chem. Phys. **127**, 227 (1988).
[9] S. Majetich, E. M. Boczar, and J. R. Weisenfeld, J. Appl. Phys. **66**, 475 (1989).
[10] S. Majetich, C. A. Tomczyk, and J. R. Weisenfeld, Phys. Rev. A **41**, 6085 (1990).
[11] *Handbook of Chemistry and Physics*, edited by D. R. Lind (CRC Press, Boca Raton, 1994).
[12] M. Musso, L. Windholz, F. Fuso, and M. Allegrini, J. Chem. Phys. **97**, 7017 (1992).
[13] SAES Getters s.p.a., Via Gallarate 215, I-20151, Milano, Italy.
[14] R. Stair, W. E. Schneider, and J. K. Jackson, Appl. Opt. **2**, 1151 (1963).
[15] A. N. Nesmeyanov, *Vapor Pressure of the Chemical Elements* (Elsevier, Amsterdam, 1963).
[16] T. Holstein, Phys. Rev. **72**, 1212 (1947).
[17] T. Holstein, Phys. Rev. **83**, 1159 (1951).
[18] A. F. Molisch, B. P. Oehry, W. Schupita, and G. Magerl, J. Quant. Spectrosc. Radiat. Transf. **49**, 361 (1993).
[19] R. I. Asadullina, N. N. Bezuglov, and E. N. Borisov, Opt. Spektrosk. **67**, 360 (1989) [Opt. Spectrosc. (USSR) **67**, 208 (1989)].
[20] A. F. Molisch, B. P. Oehry, W. Schupita, B. Sumetsberger, and G. Magerl, J. Quant. Spectrosc. Radiat. Transf. **52**, 845 (1994).
[21] T. von der Haar, C. Kramer, and M. Baumann, J. Chem. Phys. **94**, 1970 (1990).
[22] H.-P. Didra, and M. Baumann, Z. Phys. D **24**, 107 (1993).
[23] A. Bondi, J. Phys. Chem. **68**, 44 (1964).
[24] A. N. Klucharev and N. S. Rayazanov, Opt. Spektrosk. **33**, 425 (1972) [Opt. Spectrosc. (USSR) **33**, 230 (1972)].
[25] N. N. Bezuglov, A. N. Klucharev, and V. A. Sheverev, J. Phys. B **20**, 2497 (1987).